FATIGUE-CRACK PROPAGATION IN ARMOR STEELS

Albert A. Anctil, et al

Army Materials and Mechanics Research Center
Watertown, Massachusetts

November 1969

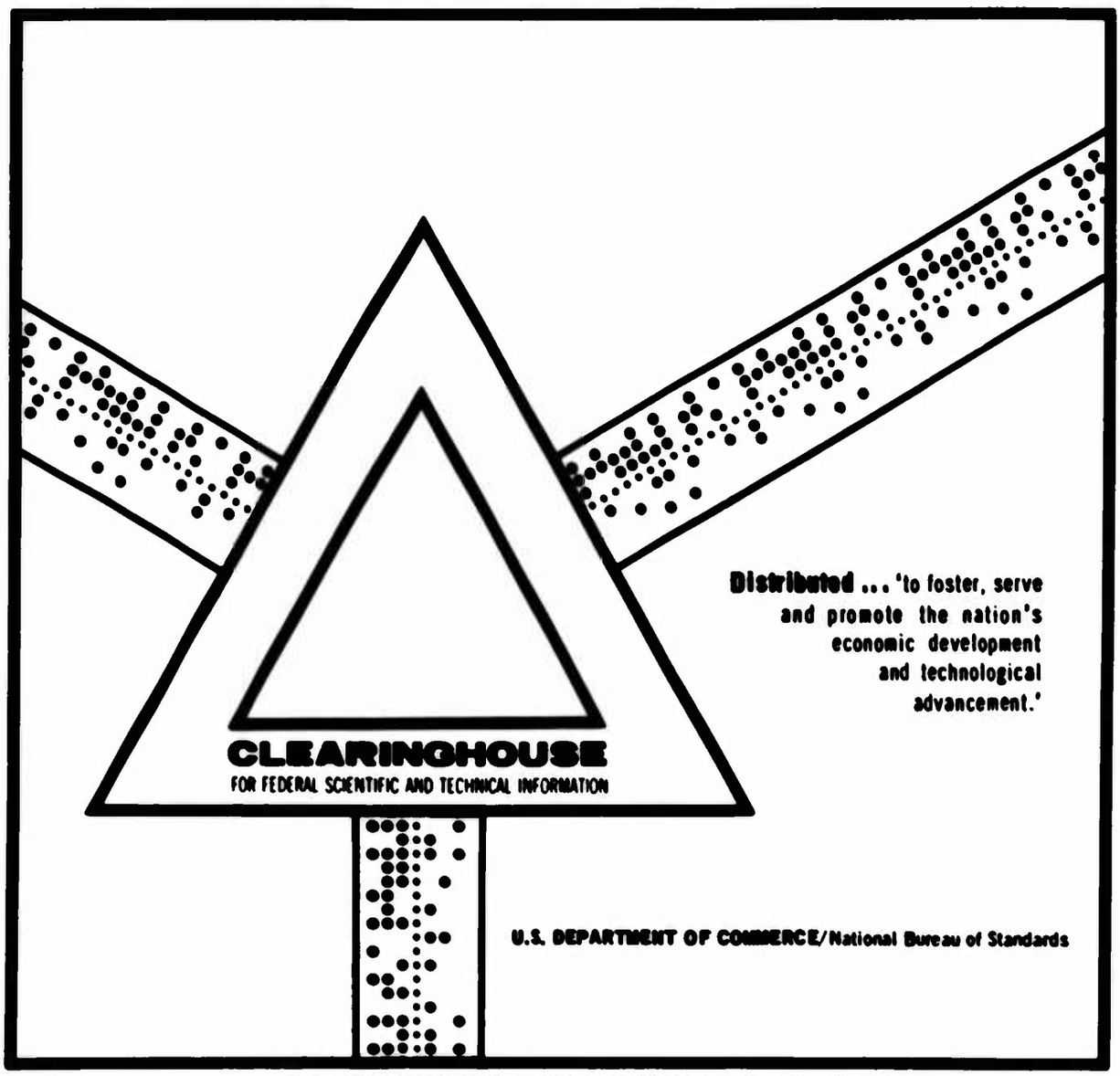

AMMRC TR 69-25

AD

FATIGUE-CRACK PROPAGATION IN ARMOR STEELS

ALBERT A. ANCTIL and ERIC B. KULA
Metals Division

November 1969

ARMY MATERIALS AND MECHANICS RESEARCH CENTER
Watertown, Massachusetts 02172

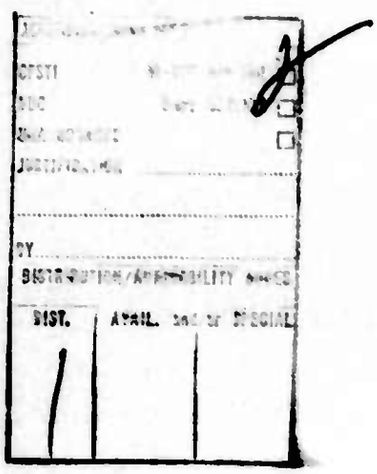

The findings in this report are not to be construed as an official Department of the Army position, unless so designated by other authorized documents.

Mention of any trade names or manufacturers in this report shall not be construed as advertising nor as an official indorsement or approval of such products or companies by the United States Government.

DISPOSITION INSTRUCTIONS

Destroy this report when it is no longer needed.
Do not return it to the originator.

AMMRC TR 69-25

FATIGUE-CRACK PROPAGATION IN ARMOR STEELS

Technical Report by

ALBERT A. ANCTIL and ERIC B. KULA

November 1969

D/A Project 1T062105A328
AMCMS Code 5025.11.294
Metals Research for Army Materiel
Subtask 39041

METALS LABORATORY
ARMY MATERIALS AND MECHANICS RESEARCH CENTER
Watertown, Massachusetts 02172

ARMY MATERIALS AND MECHANICS RESEARCH CENTER

FATIGUE-CRACK PROPAGATION IN ARMOR STEELS

ABSTRACT

Fatigue-crack propagation in high- and dual-hardness armor steels has been studied at various fatiguing stresses and testing temperatures using a fracture mechanics analysis of the data. The armor steels tested were: 1. a high-hardness XAR-30 steel; 2. an ausformed cross-rolled H11 and X27 steel composite; and 3. a dual-hardness composite of Ni-Cr-Mo steels with 0.34 and 0.51 carbon. Crack-growth rates increased directly with increasing fatiguing stress level and decreasing testing temperatures. The fatigue-crack growth rate d2a/dN versus the change in stress intensity factor ΔK followed an empirical relationship $d2a/dN = C\ \Delta K^m$ for the high-hardness and thin-section dual-hardness Ni-Cr-Mo composite steels. The crack-growth rate exponent m was 5.0 in the XAR-30 and 2.3 in the Ni-Cr-Mo steel. Crack-growth rates were generally higher in both the XAR-30 and Ni-Cr-Mo dual-hardness steels than in 4340 steel at the same strength level. The fracture mode for these steels was predominantly plane strain. The low fracture toughness component of the composite steel failed first and thereby caused rapid fatigue-crack growth acceleration and fast fracture in the remaining component.

CONTENTS

INTRODUCTION

Fatigue-crack propagation is an important factor in many failures of military components and structures. The resulting loss of life and property has prompted intensive research efforts to determine what data and analyses are required by the design engineer to overcome fatigue failures. This report presents preliminary observations and fatigue-crack growth data on through-thickness cracks for high-strength monolithic and dual-hardness armor steels. A linear elastic-fracture mechanics theory analysis of this data was utilized. This analysis uses the stress intensity factor K which describes the stress field surrounding a growing crack tip and is dependent upon the applied stress and configuration of the crack.[1] The time-history of this parameter can then be related to the fatigue-crack growth rate d2a/dN of a material and, further, may be correlated to fatigue-crack growth rate in an actual component or structure. Component or structural fatigue life can be predicted from laboratory data of ΔK versus d2a/dN curves under appropriate stress levels and environments.[2,3] Data have been reported previously on the tensile, hardness, and slow bend properties of similar armor composites, with emphasis on the bonding efficiency.[4]

MATERIALS AND PROCEDURE

The mechanical properties and chemical compositions as reported by the manufacturer are given in Table I for the steels investigated, which included a high-hardness XAR-30 steel, an ausformed composite of X27 and H11 steel, and a dual-hardness composite of a Ni-Cr-Mo steel with 0.34 and 0.51 C. Each plate tested in fatigue was 1/4-inch thick with the exception of the dual-hardness Ni-Cr-Mo steel which was also tested in a 0.033-inch thickness. The mechanical properties reported in Table I for the ausformed and Ni-Cr-Mo dual-hardness steel components were determined from thicker sections having the same thermomechanical treatment as the composite.

The pin-loaded fatigue specimens were 3.0 inches wide and 12.0 inches long. The center notch was electric-discharge machined perpendicular to the sheet rolling direction. The specimens were subjected to sinusoidal loading with a constant mean load at three cycles per second with an axial-fatigue, hydraulic, closed-loop testing machine. The specimens are identified by the applied maximum gross section stress σ_g. The minimum gross section stress in all cases was approximately 3.0 ksi. The load was measured with a strain-gaged load cell in series with the test specimen. Fatigue-crack growth was continuously followed with an electric-potential technique.[5] The change in voltage resulting from crack growth was plotted against time on an X-Y recorder. These data were then replotted as crack length 2a versus the number of cycles N for varying applied sinusoidal loads and testing temperatures. The crack-growth curves include the number of cycles necessary to initiate the fatigue crack. This procedure was satisfactory for the high-hardness XAR-30 and the 0.033-inch Ni-Cr-Mo dual-hardness composite. The two components of the 0.25-inch-thick composites fatigue individually. Crack initiation occurs nearly simultaneously in both components of the composite.

Table I. MECHANICAL PROPERTIES AND CHEMICAL COMPOSITION

Armor Steel	Material	Thickness (in.)	Mechanical Properties						
			Y.S. ksi 0.1%	Y.S. ksi 0.2%	T.S. ksi	Elon. %	R.A. %	Hardness R_c	Fracture Toughness K_c-ksi$\sqrt{in.}$
High-Hardness	XAR-30	0.25	170	192	255	8.5	35.0	53	-
Ausformed	X27	.30	200	220	289	9.0	-	50	-
	X11	.30	233	258	349	7.0	-	57	-
Dual-Hardness Ni-Cr-Mo	.34 C	.25	-	183	262	9.0	45.0	51	63
	.51 C	.25	-	219	361	6.0	15.0	61	28
	Composite	.40	-	185	319	9.0	12.0	-	-

	Chemical Composition, Weight %									
		C	Mn	Si	Ni	Cr	Mo	V	P	S	Misc.
	XAR-30	0.32	0.93	0.61	0.06	0.59	0.18	-	0.007	0.028	0.13 Zr
	X27	.28	.67	.35	3.28	1.02	2.06	0.10	-	-	-
	H11	.39	.20	.96	-	4.75	1.32	.51	-	-	-
	.34 C	.34	.79	.31	1.03	0.47	0.46	-	.005	.007	.024 Al
	.51 C	.51	.63	.27	1.04	0.51	0.47	-	.006	.008	.031 Al
	Composite	-	-	-	-	-	-	-	-	-	-

However, the rate of fatigue-crack growth is considerably higher in the higher strength, lower fracture toughness component. Therefore, the 2a versus N curves represent an average crack length versus the number of cycles for these composites.

Crack-growth rates d2a/dN were determined graphically from the 2a versus N curves. The stress intensity factor was calculated from $K = \sigma_g \sqrt{a}\ \alpha$ where σ_g is the gross section stress and "a" is one-half the crack length. The term α relates the crack length and geometric variables to correct for the finite width of the specimen as $2a \geq W/2$. The analysis of Isida was used to determine α.[6] Although crack lengths were measured up to fracture, crack-growth rates were determined only up to a maximum crack length of 2.1 inches, since beyond this length the calculation of K becomes increasingly inaccurate.

The quantity ΔK is then the difference between the stress intensity factor at the maximum load and at the minimum load at a particular crack length. The crack propagation rate for the accumulation of fatigue damage was related to ΔK by the empirical power law relationship as proposed by Paris:[2] $d2a/dN = C\ (\Delta K)^m$ where C and m are constants.

RESULTS

High-Hardness Steel

The high-hardness XAR-30 steel was austenitized at 1650 F and was spray-water quenched resulting in a tensile strength of 255 ksi. The fractographs are shown in Figure 1 for specimens tested at room temperature at σ_g values of 12.3, 19.7, and 24.6 ksi. It was observed that fatigue-crack growth occurred under plane strain conditions and was not symmetrical. The fatigue fracture appearance becomes coarser with increasing σ_g and the fast fracture regions have ductile shear lips. The fractograph for Specimen 2 is a cross section of the pinhole area where fatigue initiated at two flaw sites located in the upper right and lower left sections of the pinhole perpendicular to the applied stress. The darker region adjacent to the machined notch in Specimen 3 is a pop-in. The pop-in phenomenon, or rapid internal extension of the crack front, occurred at a plane strain critical stress intensity value of 31.1 ksi $\sqrt{in.}$ after approximately 250 cycles.

Figure 1. Room temperature fractographs of high hardness XAR-30 steel fatigued at σ_g values of 12.3 ksi (Specimen 1), 19.7 ksi (Specimen 2), and 24.6 ksi (Specimen 3). Mag. 2.2X

The crack-growth curves are shown in Figure 2a. Doubling σ_g reduced the fatigue life 66.0 percent. Crack-growth data is shown for σ_g = 19.7 ksi (Specimen 2) to the point where the center notch crack arrested itself. Fatigue-crack growth continued in the specimen pinhole. Stress intensity factors at fracture are not reported because the crack lengths reached are beyond the fracture mechanics analysis.

The crack-growth rate was measured at various points on each crack-growth curve and plotted versus the change in stress intensity factor about the growing crack tip on log-log coordinates. These are shown in Figure 3. The data for each specimen follow the empirical power law relationship with the exponent equal to 5.0. This value of the exponent is higher than the values of 2.5 to 4.0 reported in the literature for tempered steel but it is not too surprising for this steel in the as-quenched or lightly tempered condition.[7]

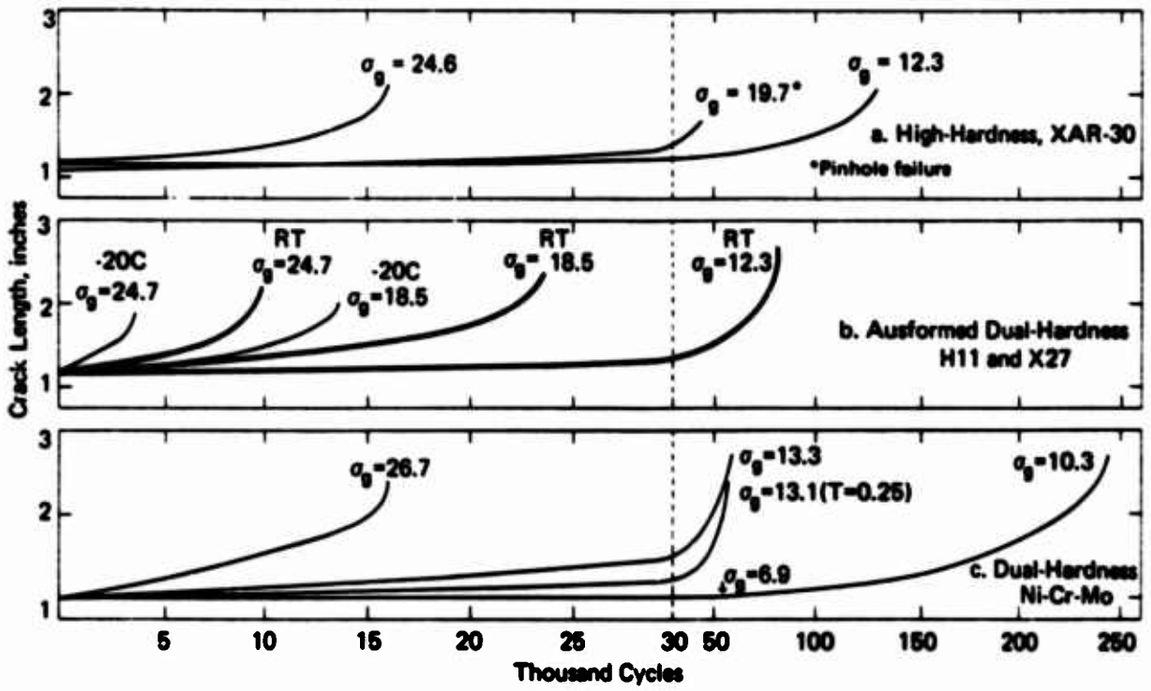

Figure 2. Crack length versus the number of cycles

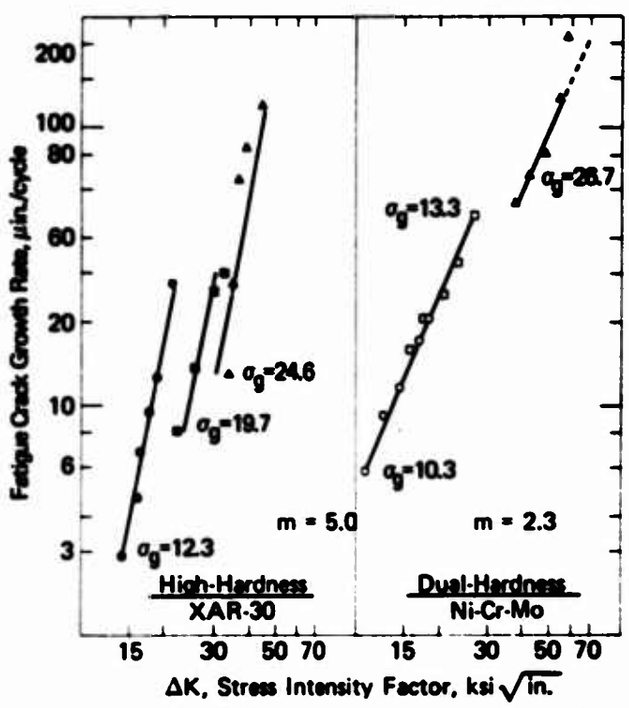

Figure 3. Fatigue crack growth rates versus the stress intensity factor range

Although the data follow the relationship at a particular σ_g, there is a lateral displacement to higher values of stress intensity factors as σ_g is increased. Generally, crack-growth rates measured at different crack lengths on samples with different gross stresses fall on one curve; however, that is not the behavior shown here. One exception has been noted when the ratio of the maximum to the minimum gross stress during cycling is low, approaching one. For the three tests shown in Figure 3 this ratio varies from 4 for σ_g = 12.3 to 8 for σ_g = 24.6 ksi. However, the deviations usually noted at low values of this ratio are such that higher values of ΔK are needed for an equivalent rate of crack growth. This is opposite to the behavior noted here. The reason for the behavior in Figure 3 is unexplained.

Ausformed Dual-Hardness Steel

The ausformed steel composite consisted of equal thickness plates of X27 and H11 steel. This composite had been austenitized at 1900 F, quenched into the austenite bay region at 1500 F where it was cross-rolled with a 54 percent reduction and then quenched to form martensite. This was followed with a two-hour temper at 400 F. The X27 steel had a tensile strength of 289 ksi and the H11 steel a tensile strength of 349 ksi, as determined on monolithic samples processed similarly (Table I).

The fractographs for these composites are shown in Figure 4. The upper portion in each specimen is the H11 steel. The first three specimens were tested at room temperature at σ_g values of 12.3, 18.5, and 24.7 ksi. These stresses are 6, 8, and 11 percent of the tensile yield strength of the X27 steel. Curves for the average crack growth versus the number of cycles for these specimens are shown in Figure 2b. The fatigue life for σ_g of 12.3 ksi was 82,000 cycles. Raising the stress 50 percent to 18.5 ksi resulted in a 70 percent reduction from this fatigue life, while a 100 percent increase in stress, or 24.7 ksi, reduced the life 88 percent.

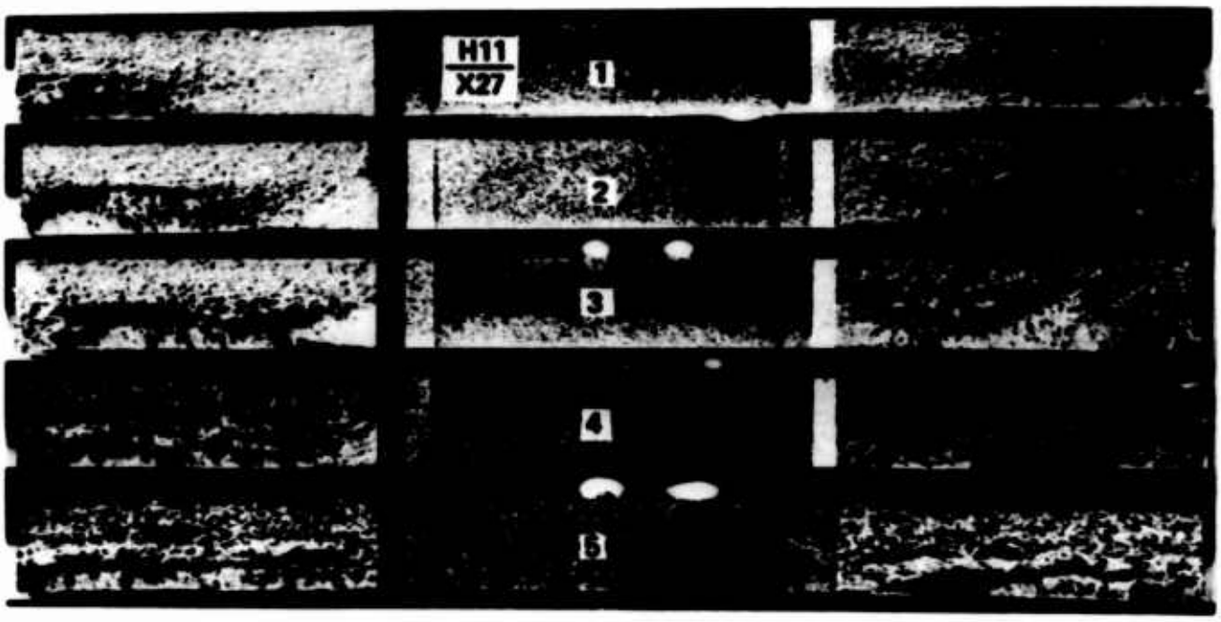

Figure 4. Fractographs of ausformed H11 and X27 steel composites. Specimens 1, 2, and 3 were fatigued at +24C and at σ_g values of 12.3, 18.5, and 24.7 ksi. Specimens 4 and 5 were fatigued at -20C with σ_g equal to 18.5 and 24.7 ksi. Mag. 2.2X

From the fractographs in Figure 4 and from observations during testing, it was clear that the fatigue crack initiates in both components. The crack-growth rate in the H11 is faster than in the X27 steel, however. The crack grows in the H11 as a flat fracture, under plane strain conditions, until this portion of the composite has failed completely. Simultaneously, the

crack length in the X27 steel is increasing as the net section stress increases, until the material fails at a net section stress approximately equal to 50 percent of the tensile yield strength. The fast fracture in the X27 is ductile with a full shear lip. The crack length at which final fast fracture initiates in the X27 steel is less the higher the gross stress during fatiguing. Approximate stress intensity factors at failure for the X27, using a value of σ_g double the applied stress, since the H11 is not supporting the load, are 75.0, 92.0, and 90.0 ksi $\sqrt{in.}$ Some evidence of delamination at the interface is evident at the largest crack lengths.

Specimens 4 and 5 were tested at -20 C in dry ice and ethyl alcohol with σ_g values of 18.5 and 24.7 ksi. The fatiguing and fracturing sequence was the same as at room temperature. The coarser structure in the H11 indicates the faster crack-growth rate over the room temperature tests. A decrease in fatigue life of 43 and 64 percent, as compared to room temperature tests, occurred. This reduction is shown in the crack-growth curves in Figure 2b. The fracture toughness was lowered for the composite at -20 C and the approximate stress intensity factors for the X27 steel at failure were reduced to 60.0 and 75.0 ksi $\sqrt{in.}$ at σ_g values of 18.5 and 24.7 ksi, respectively.

Dual-Hardness Steel

The chemical compositions of the heat-treatable steels used in this composite are essentially the same except for the carbon content. The component containing 0.34 C has a tensile strength of 262 ksi and plane strain fracture toughness stress intensity factor K_{Ic} of 63.0 ksi $\sqrt{in.}$, while the 0.51 C component has a tensile strength of 361 ksi and a K_{Ic} value of 28 ksi $\sqrt{in.}$

The dual-hardness composite was oil-quenched from 1500 F and double tempered at 250 F for one hour. Two thicknesses, 0.033 and 0.250 inch, were tested. The fractographs for the room temperature tests are shown in Figure 5. Again the fatiguing sequence was the same as for the ausformed composites. However, due to the bowed condition of Specimen 1 over its length, initiation and some crack growth did occur first in the 0.34 C component. This amount of growth can be seen on the fracture surface as the first dark band extending through the thickness. The crack-growth rate then decreased significantly and the rate in the higher strength 0.51 C steel, accelerated to failure (left cross section). This was followed by rapid fracturing of the remaining cross section. The crack-growth curve is shown in Figure 2c. The 0.250-inch thick composite has the same fatigue life as a thinner composite measuring 0.033 inch at the same gross stress. Specimen 2, σ_g = 20.1 ksi, and Specimen 3, σ_g = 25.4 ksi, failed during fatiguing (right cross section) at pinhole machining flaws in the high-strength 0.51 C component. Some fatigue-crack growth took place in the 0.31 C component in Specimen 2.

Specimens 4, 5, and 6 measured 0.033-inch thick. Fatigue-crack growth in these thin-section composites was through the thickness with a full shear development during fatigue and fast fracture. This allowed measurements to be made of the fatigue-crack length during testing. A maximum stress of 6.9 ksi, which is 3.8 percent of the tensile yield strength of the 0.34 C

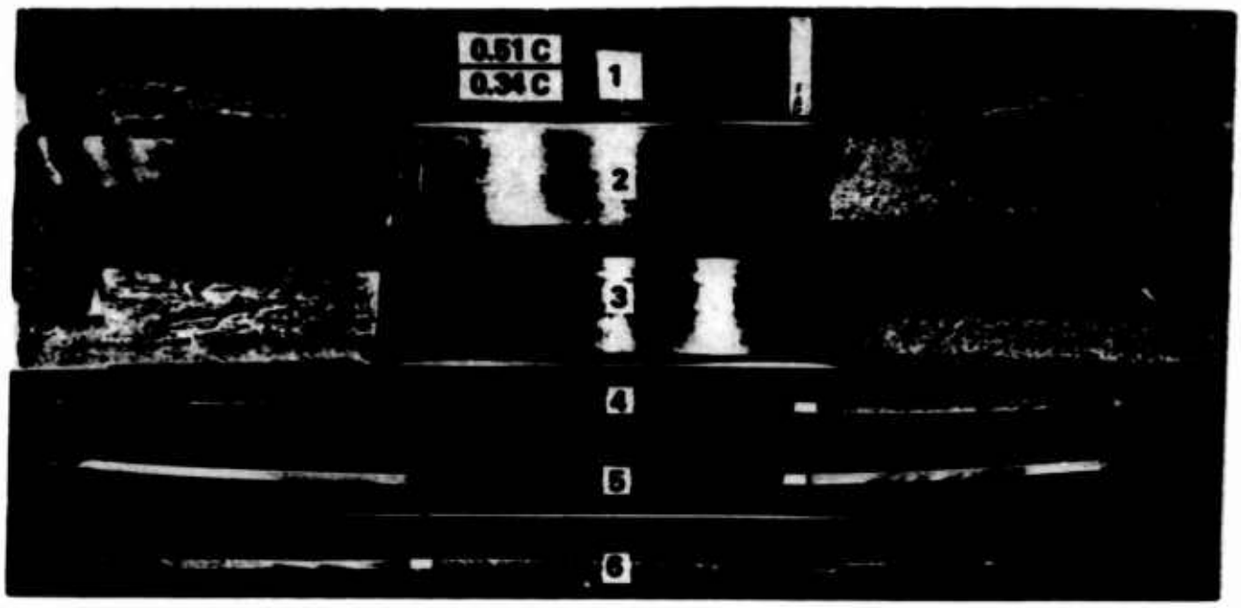

Figure 5. Room temperature fractographs of dual hardness Ni-Cr-Mo steel composites fatigued (top to bottom) at the following σ_g values: 13.1, 20.1, 25.4, 6.9 increased to 10.3, 13.3, and 26.7 ksi. Specimens 2 and 3 failed in the pinhole. Mag. 2.2X

component, was used to initiate the fatigue crack in 50 x 10^3 cycles in Specimen 4. This was done to illustrate the magnitude of stresses required for fatigue-crack initiation. The stress on this specimen was then raised to 10.3 ksi where it accumulated an additional 190,000 cycles before failing. Fatigue stresses of 13.3 and 26.7 ksi were applied to Specimens 5 and 6. The crack-growth curves in Figure 2c show a 72 percent decrease in fatigue life when the gross section stress is doubled from 13.3 to 26.7 ksi. The fatigue-crack growth rates versus the change in stress intensity for these three specimens are plotted in Figure 3. The data for these composites also follow the power law relationship with 2.3 as the exponent. As with the high-hardness XAR-30, the data from the several tests do not all fall on one straight line. The exponent is one-half that reported for the high-hardness XAR-30 steel. However, when comparing the crack-growth rates over small changes in stress intensity factors, 10-20 ksi $\sqrt{\text{in.}}$, the dual-hardness steel is fatiguing at a faster rate than the XAR-30 steel.

DISCUSSION

Perhaps the most important question is how the fatigue-crack growth rate in these armor steels compares with other steels. Unfortunately, this is not a question which can be answered unequivocally. As has been stated earlier, crack-growth rates under sinusoidal loading generally follow a power law relationship of the form $d2a/dN = C\ (\Delta K)^m$. Deviation from the power law relationship may be noted at very short crack lengths during the initiation stage,

when growth rates are smaller than predicted or below some threshold value of ΔK. Deviation also occurs at very large crack lengths where instability is approached, when the crack-growth rate accelerates and final fast fracture occurs. Other factors, such as environment, sample thickness and width, frequency of loading, etc., also influence the behavior to varying and unknown degrees. But under controlled laboratory conditions, crack-growth rates for different materials can be compared.

Since both the coefficient C and the crack-growth rate exponent m in the above equation vary with material, curves of crack-growth rate versus ΔK for different materials intersect. Therefore, the relative susceptibility to fatigue-crack growth depends on the stress intensity range considered. This is illustrated in Figure 6, where the curves of Figure 3 are replotted together with typical data for 4340 steel, quenched, and tempered over the range 400 to 700 F.[7] It can be seen that over much of the range, the dual-hardness Ni-Cr-Mo steel and the high-hardness XAR-30 steel have a higher crack-growth rate than the high-strength 4340 steel. The crack-growth exponent for the XAR-30 steel, 5.0, is much higher than for the 4340 steel, which averaged about 2.6. On the other hand, the exponent for the dual-hardness Ni-Cr-Mo steel was slightly lower than for the 4340. The exponents for both armor steels are somewhat suspect however, since the data from the different specimens do not fall on one straight line.

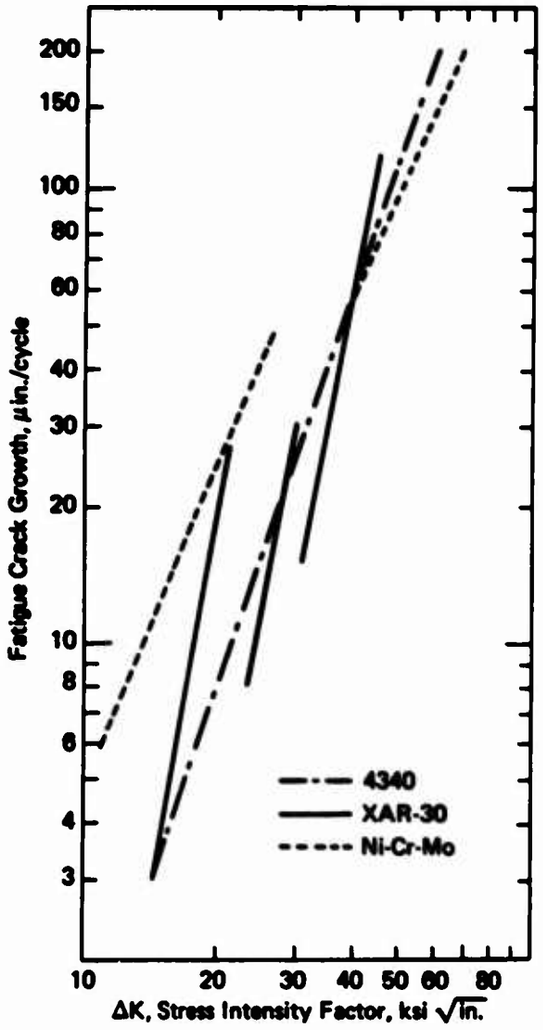

Figure 6. Fatigue crack growth rates versus the stress intensity factor range

An additional factor of importance not investigated here is the fracture toughness, which limits the actual crack length that can be tolerated without rapid fracture. The fracture toughness of these materials at the investigated hardness levels is probably quite low.

The type of crack considered in this investigation is a through-thickness crack. The major reason for its selection is the ease of preparation and study. Other types of cracks which would be of interest include a partial thickness crack, through the hard component of the dual-hardness armor, and a delamination, or separation, of the two components along the interface.

The through-thickness crack considered here does have some basis in reality, since it is the type crack which would grow from a bolt hole (as in Figures 1 and 3) or a hole from penetration by a projectile.

Growth of a fatigue-crack in a composite material such as the dual-hardness armor poses some interesting problems. The crack resistance of the dual-hardness armor depends on the properties of each component of the composite, its thickness, and presumably the efficiency of the bond between the two components. By making some simplifying assumptions, it is possible to qualitatively explain some of the behavior shown by dual-hardness composites.

Of particular interest is the influence of stress level on the course of the fatigue-crack growth in the dual-hardness ausformed H11 and X27 composite shown in Figure 4. The crack initiates in both components, but it grows more rapidly in the higher hardness H11 steel. When the crack has grown completely through the H11, the higher net section stress on the remaining portion of uncracked X27 causes the crack-growth rate to accelerate and fast fracture to occur. The crack length in the X27 at which this occurs decreases with increasing gross section stress σ_g; that is, the higher the value of σ_g, the more the crack growth in the X27 lags that in the H11.

Assumed crack-growth rates as a function of ΔK for monolithic samples of H11 and X27 are shown schematically in Figure 7. At a given crack length and σ_g, the growth rate in the H11 is greater than that in the X27. As fatiguing progresses and ΔK increases, the rate of crack growth increases faster in the H11 than in the X27, since not only does the curve for H11 lie above that for X27, but it has a higher crack-growth rate exponent so that the curves diverge. Increasing the initial gross section stress σ_g simply starts the crack growth process at a higher value of ΔK. Accordingly, the initial difference in crack-growth rates between the two materials is greater than for a lower stress, and when the H11 has failed, the total crack length in the X27 is less.

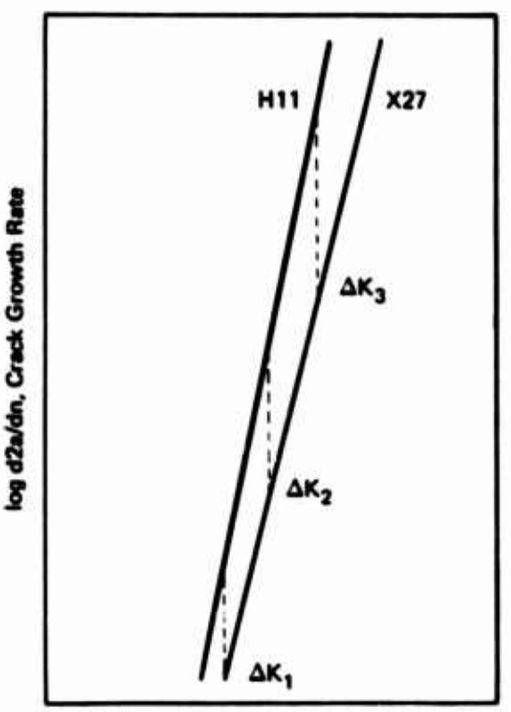

Figure 7. Assumed crack growth rates versus the stress intensity factor range for monolithic components

While this grossly simplified picture can explain in a qualitative way the effect of crack-growth rate exponent and initial gross section stress, it assumes that the two components of the composite are fatiguing completely independently. In an actual composite, there would undoubtedly be some load transfer from the material

with the longer crack to that with the shorter, so that the difference in crack-growth rates would be less than assumed here. Furthermore, there is an effect of thickness, for example, the 0.033-inch-thick dual-hardness Ni-Cr-Mo steel fatigued as a homogeneous structure. Finally, the efficiency of the bond between the two components should have some effect. Some of these factors are currently under investigation.

SUMMARY

Fatigue-crack growth has been studied in three armor steels: a) high-hardness XAR-30 steel; b) an ausformed H11 and X27 steel composite; and c) a dual-hardness composite of Ni-Cr-Mo steels with 0.34 and 0.51 percent carbon. Center-notched specimens with through-thickness cracks were used.

Crack-growth rates increased directly with increasing fatiguing stress level and decreasing test temperature. The data generally conformed to an empirical relationship of the form $d2a = C (\Delta K)^m$. The crack-growth rate exponent m was 5.0 in the XAR-30 steel and 2.3 in the Ni-Cr-Mo steel. Crack-growth rates were generally higher in both the XAR-30 and Ni-Cr-Mo dual-hardness steels than in 4340 steel at the same strength level.

Observations of the fracture surfaces showed that the fatigue fracture was predominantly flat, plane strain. In the 0.25-inch-thick dual-hardness composites, the fatigue crack initiated in both components, but grew faster in the higher strength, lower fracture toughness component. After this component failed there was an acceleration of the growth rate in the lower strength component and fast fracture finally occurred. The crack length in the low-strength component at which fast fracture occurred was smaller the higher the initial fatiguing stress level. This effect of stress level can qualitatively be explained by assuming that the growth rate and the growth exponent are higher in the higher strength component.

ACKNOWLEDGMENT

The authors wish to thank Mr. R. Swanson for carrying out the experimental phase, and Mr. D. Papetti for his technical assistance and cooperation in obtaining these composite materials.

LITERATURE CITED

1. IRWIN, G. R. *Analysis of Stresses and Strains Near the End of a Crack Traversing a Plate.* Transactions Am. Soc. Mechanical Engrs., v. 79, 1957, p. 361.

2. PARIS, P. C. *The Fracture Mechanics Approach to Fatigue, Fatigue - An Interdisciplinary Approach.* Syracuse University Press, New York, 1964, p. 107.

3. TIFFANY, C. F., and MASTERS, J. N. *Fracture Toughness Testing and its Applications.* Am. Soc. Testing Mats., STP 381, 1965, p. 249.

4. HICKEY, C. F. *Mechanical Properties and Bonding Efficiency of Steel Composites.* Army Materials and Mechanics Research Center, AMMRC TR 67-12, May 1967; also Am. Soc. Testing Mats., Journal of Mats., v. 3, 1968, p. 3.

5. ANCTIL, A. A., KULA, E. B., and DiCESARE, E. *Electric Potential Technique for Determining Slow Crack Growth.* Army Materials and Mechanics Research Center, AMRA TR 63-27, December 1963; also Proceedings Am. Soc. Testing Mats., v. 63, 1963, p. 799.

6. ISIDA, M. *K Calibration, Plane Strain Crack Toughness Testing.* Am. Soc. Testing Mats., STP 410, 1966, p. 11.

7. ANCTIL, A. A., and KULA, E. B. *Fatigue-Crack Propagation in 4340 Steel as Affected by Tempering Temperature.* Army Materials and Mechanics Research Center, AMMRC TR 69-15, June 1969.

UNCLASSIFIED
Security Classification

DOCUMENT CONTROL DATA - R&D
(Security classification of title, body of abstract and indexing annotation must be entered when the overall report is classified)

1. ORIGINATING ACTIVITY (Corporate author) Army Materials and Mechanics Research Center Watertown, Massachusetts 02172	2a. REPORT SECURITY CLASSIFICATION Unclassified 2b. GROUP

3. REPORT TITLE

FATIGUE-CRACK PROPAGATION IN ARMOR STEELS

4. DESCRIPTIVE NOTES (Type of report and inclusive dates)

5. AUTHOR(S) (Last name, first name, initial)

Anctil, Albert A. and Kula, Eric B.

6. REPORT DATE November 1969	7a. TOTAL NO. OF PAGES 14	7b. NO. OF REFS 7
8a. CONTRACT OR GRANT NO. b. PROJECT NO. D/A 1T062105A328 c. AMCMS Code 5025.11.294 d. Subtask 39041	9a. ORIGINATOR'S REPORT NUMBER(S) AMMRC TR 69-25 9b. OTHER REPORT NO(S) (Any other numbers that may be assigned this report)	

10. AVAILABILITY/LIMITATION NOTICES

This document has been approved for public release and sale; its distribution is unlimited.

11. SUPPLEMENTARY NOTES	12. SPONSORING MILITARY ACTIVITY U. S. Army Materiel Command Washington, D. C. 20315

13. ABSTRACT

Fatigue-crack propagation in high- and dual-hardness armor steels has been studied at various fatiguing stresses and testing temperatures using a fracture mechanics analysis of the data. The armor steels tested were: 1. a high-hardness XAR-30 steel; 2. an ausformed cross-rolled H11 and X27 steel composite; and 3. a dual-hardness composite of Ni-Cr-Mo steels with 0.34 and 0.51 carbon. Crack-growth rates increased directly with increasing fatiguing stress level and decreasing testing temperatures. The fatigue-crack growth rate d2a/dN versus the change in stress intensity factor ΔK followed an empirical relationship $d2a/dN = C\,\Delta K^m$ for the high-hardness and thin-section dual-hardness Ni-Cr-Mo composite steels. The crack-growth rate exponent m was 5.0 in the XAR-30 and 2.3 in the Ni-Cr-Mo steel. Crack-growth rates were generally higher in both the XAR-30 and Ni-Cr-Mo dual-hardness steels than in 4340 steel at the same strength level. The fracture mode for these steels was predominantly plane strain. The low fracture toughness component of the composite steel failed first and thereby caused rapid fatigue-crack growth acceleration and fast fracture in the remaining component. (Authors)

DD FORM 1 JAN 64 1473

UNCLASSIFIED
Security Classification

14. KEY WORDS	LINK A		LINK B		LINK C	
	ROLE	WT	ROLE	WT	ROLE	WT
Steel composites Composite armor Fatigue cracking Fracture properties Crack propagation Toughness						

INSTRUCTIONS

1. **ORIGINATING ACTIVITY:** Enter the name and address of the contractor, subcontractor, grantee, Department of Defense activity or other organization *(corporate author)* issuing the report.

2a. **REPORT SECURITY CLASSIFICATION:** Enter the overall security classification of the report. Indicate whether "Restricted Data" is included. Marking is to be in accordance with appropriate security regulations.

2b. **GROUP:** Automatic downgrading is specified in DoD Directive 5200.10 and Armed Forces Industrial Manual. Enter the group number. Also, when applicable, show that optional markings have been used for Group 3 and Group 4 as authorized.

3. **REPORT TITLE:** Enter the complete report title in all capital letters. Titles in all cases should be unclassified. If a meaningful title cannot be selected without classification, show title classification in all capitals in parenthesis immediately following the title.

4. **DESCRIPTIVE NOTES:** If appropriate, enter the type of report, e.g., interim, progress, summary, annual, or final. Give the inclusive dates when a specific reporting period is covered.

5. **AUTHOR(S):** Enter the name(s) of author(s) as shown on or in the report. Enter last name, first name, middle initial. If military, show rank and branch of service. The name of the principal author is an absolute minimum requirement.

6. **REPORT DATE:** Enter the date of the report as day, month, year; or month, year. If more than one date appears on the report, use date of publication.

7a. **TOTAL NUMBER OF PAGES:** The total page count should follow normal pagination procedures, i.e., enter the number of pages containing information.

7b. **NUMBER OF REFERENCES:** Enter the total number of references cited in the report.

8a. **CONTRACT OR GRANT NUMBER:** If appropriate, enter the applicable number of the contract or grant under which the report was written.

8b, 8c, & 8d. **PROJECT NUMBER:** Enter the appropriate military department identification, such as project number, subproject number, system numbers, task number, etc.

9a. **ORIGINATOR'S REPORT NUMBER(S):** Enter the official report number by which the document will be identified and controlled by the originating activity. This number must be unique to this report.

9b. **OTHER REPORT NUMBER(S):** If the report has been assigned any other report numbers *(either by the originator or by the sponsor)*, also enter this number(s).

10. **AVAILABILITY/LIMITATION NOTICES:** Enter any limitations on further dissemination of the report, other than those imposed by security classification, using standard statements such as:

(1) "Qualified requesters may obtain copies of this report from DDC."

(2) "Foreign announcement and dissemination of this report by DDC is not authorized."

(3) "U. S. Government agencies may obtain copies of this report directly from DDC. Other qualified DDC users shall request through _____."

(4) "U. S. military agencies may obtain copies of this report directly from DDC. Other qualified users shall request through _____."

(5) "All distribution of this report is controlled. Qualified DDC users shall request through _____."

If the report has been furnished to the Office of Technical Services, Department of Commerce, for sale to the public, indicate this fact and enter the price, if known.

11. **SUPPLEMENTARY NOTES:** Use for additional explanatory notes.

12. **SPONSORING MILITARY ACTIVITY:** Enter the name of the departmental project office or laboratory sponsoring *(paying for)* the research and development. Include address.

13. **ABSTRACT:** Enter an abstract giving a brief and factual summary of the document indicative of the report, even though it may also appear elsewhere in the body of the technical report. If additional space is required, a continuation sheet shall be attached.

It is highly desirable that the abstract of classified reports be unclassified. Each paragraph of the abstract shall end with an indication of the military security classification of the information in the paragraph, represented as *(TS), (S), (C), or (U).*

There is no limitation on the length of the abstract. However, the suggested length is from 150 to 225 words.

14. **KEY WORDS:** Key words are technically meaningful terms or short phrases that characterize a report and may be used as index entries for cataloging the report. Key words must be selected so that no security classification is required. Identifiers, such as equipment model designation, trade name, military project code name, geographic location, may be used as key words but will be followed by an indication of technical context. The assignment of links, rules, and weights is optional.